ISBN: 978-3-95450-234-9 ISSN: 2673-5504 doi:10.18429/JACoW-SRF2023-MOIXA04

OPERATIONAL EXPERIENCE FOR RIKEN SUPERCONDUCTING LINEAR ACCELERATOR

K. Yamada*, M. Fujimaki, H. Imao, O. Kamigaito, M. Komiyama, K. Kumagai, T. Nagatomo, T. Nishi, H. Okuno, K. Ozeki, N. Sakamoto, K. Suda, A. Uchiyama, T. Watanabe, Y. Watanabe
RIKEN Nishina Center, Wako, Japan

Abstract

The RIKEN superconducting heavy-ion linac, SRILAC, has been successfully operating for almost four years and has stably delivered heavy-ion beams for super-heavy-element synthesis experiments. SRILAC consists of ten superconducting (SC) quarter-wavelength resonators made from pure Nb sheets that operate at 4.5 K. The effects of a broken coupler during the initial operation and after four years of operation resulted in increased X-ray emission levels in several superconducting cavities. Recently, we found that field emissions can be significantly reduced with high-voltage pulse conditioning. We are also preparing ten new couplers and two spare superconducting cavities to permanently solve this problem. This article shares the lessons learned from experiences in a four-year operation with low-beta SC cavities.

INTRODUCTION

The Radioactive Isotope Beam Factory (RIBF) [1, 2] at the RIKEN Nishina Center began operations in 2006. The aim was to pursue heavy-ion beam science through basic and applied research, such as determining the origin of the elements, establishing new nuclear models, synthesizing new elements and isotopes, researching nuclear transmutation, and supporting industrial applications, including the biological breeding and production of useful RIs. Figure 1 shows a schematic of the RIBF. The RIBF can provide an intense RI beam for all masses by accelerating heavy-ion beams up to 70% of light speed in cw mode, using a cascade of four separate-sector cyclotrons: the RIKEN ring cyclotron (RRC [3], K = 540 MeV), the fixed-frequency ring cyclotron (fRC [4–6], K = 700 MeV), the intermediate-stage ring cyclotron (IRC [7], K = 980 MeV), and the world's first superconducting ring cyclotron (SRC [8], K = 2600 MeV). The cyclotron cascade is combined with different types of injectors: a variable-frequency heavy-ion linac (RILAC [9, 10]), fixed-frequency heavy-ion linac (RILAC2 [11, 12]), and K70-MeV AVF cyclotron (AVF [13]). RILAC is used as an injector for medium-mass ions such as ^{48}Ca, RILAC2 for very heavy ions such as xenon and uranium, and AVF for light-mass ions. RILAC and AVF were also operated in stand-alone mode. In particular, RILAC plays a crucial role in providing high-intensity beams for superheavy elements (SHEs) experiments. Nihonium, the first element discovered in Japan, was synthesized [14] using a beam supplied by RILAC.

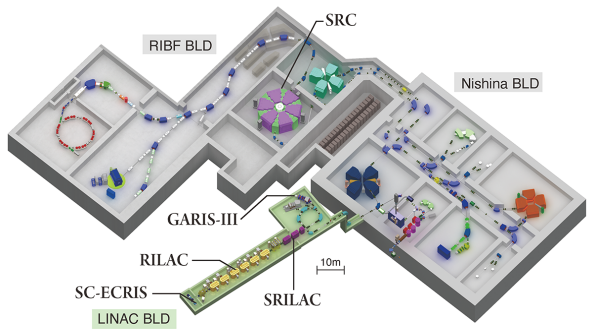

Figure 1: Schematic of the RIBF at RIKEN Nishina Center. The linac facility described in this article is shown in the lower part of the figure.

After the discovery of nihonium in the old linac facility, the facility was upgraded [15] to increase the beam intensity and energy for synthesizing new SHEs above $Z = 118$ and to produce valuable RIs such as ^{211}At. For the upgrade, we constructed a new superconducting ECR ion source [16] to obtain a higher beam intensity and introduced a superconducting booster linac named SRILAC to increase the beam energy in a limited space, as shown in Fig. 2. The goal of the RILAC upgrade project was to accelerate ions with $m/q = 6$ to 6.5 MeV/u. The budget was approved in fiscal year 2016, and construction was completed in 2019.

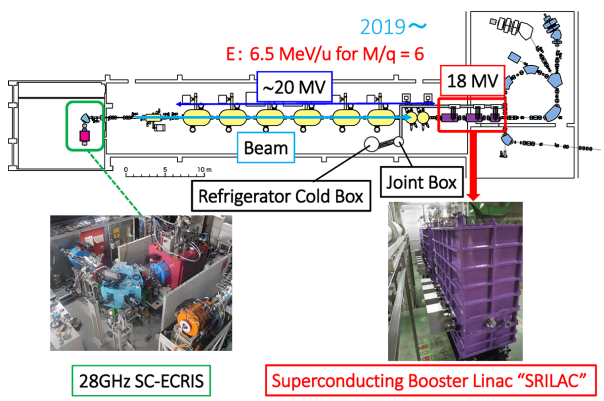

Figure 2: Schematic of the heavy-ion linac facility at RIKEN after the upgrade. The eight tanks shown in yellow are the existing room-temperature drift-tube linac, RILAC.

* nari-yamada@riken.jp

ISBN: 978-3-95450-234-9 ISSN: 2673-5504 doi:10.18429/JACoW-SRF2023-MOIXA04

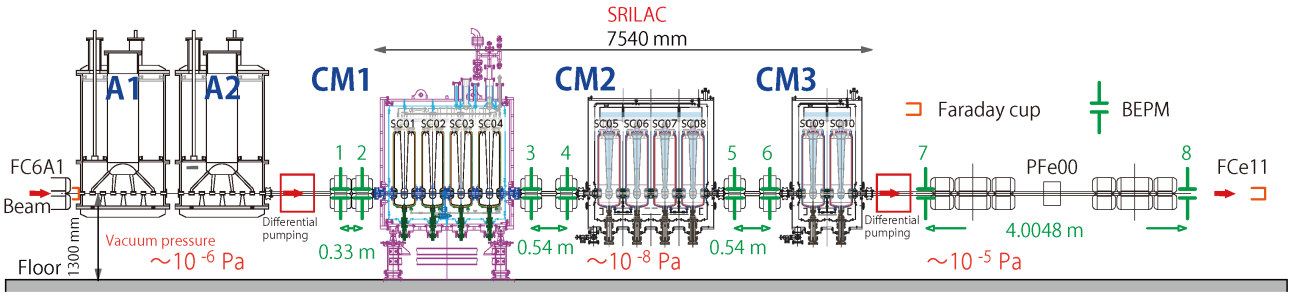

Figure 3: Layout of the SRILAC. A beam-energy and position monitor (BEPM) was installed inside each quadrupole magnet. A wire scanner (PFe00) and Faraday cup (FCe11) were installed at the HEBT downstream of the SRILAC. A pair of differential pumping systems were installed at the boundary between the SRILAC and the existing warm section.

OVERVIEW OF SRILAC

The layout of SRILAC [17] is illustrated in Fig. 3. The maximum voltage gain of the SRILAC was set to 18 MV to provide a beam energy margin. To achieve this, we fabricated ten superconducting quarter-wavelength resonators (SC-QWRs, SC01–SC10) stored in three cryomodules (CMs, CM1–CM3). The two upstream cryomodules (full-CM) contained four SC-QWRs, and the downstream cryomodule (half-CM) contained two SC-QWRs. The resonant frequency was set to 73 MHz, which was the fourth harmonic of the fundamental frequency of the RIBF. The operational temperature of the CM was 4.5 K using a liquid-helium refrigerator HELIAL MF manufactured by Air Liquide S.A. We fabricated one prototype and ten actual cavities using RRR = 250 pure niobium sheets supplied by Tokyo Denkai Co., Ltd. Surface treatment was performed sequentially based on buffered chemical polishing (BCP):110 μm BCP, ultrasonic cleaning with pure water, annealing at 750 °C for 3 h, 20 μm BCP, ultrasonic cleaning with detergent, rinsing with pure water, high-pressure rinsing (HPR) with 8 MPa ultrapure water, and baking at 120 °C for 48 h. To reduce the complexity in assembling the cryomodules, a magnetic shield was placed in a titanium helium vessel. The SRILAC complies with the High-Pressure Gas Safety Act of Japan. A schematic of the full-CM and SC-QWR for the SRILAC is shown in Fig. 4.

Room temperature quadrupole magnets were used as the focusing elements of the SRILAC. Nondestructive beam monitors (BEPMs) were developed and installed to measure the beam energy and position in the cold section [18] in each quadrupole between cryomodules and at the downstream of SRILAC. The monitor is based on a capacitive pickup with a pair of parabolic-cut electrodes. The beam energy can be deduced using the time-of-flight between the two BEPMs. In the HEBT, we used a wire scanner and a Faraday cup. One of the most concerning issues in the upgrade was that the cryomodule had to be connected to a dirty beamline built decades ago. Since the vacuum levels of those beamlines are ten to -5 or -6 Pa order, it is necessary to prevent the gas flow from the room temperature section. Therefore, we developed a three-stage differential pumping system and installed it [19] on each side of the cold section.

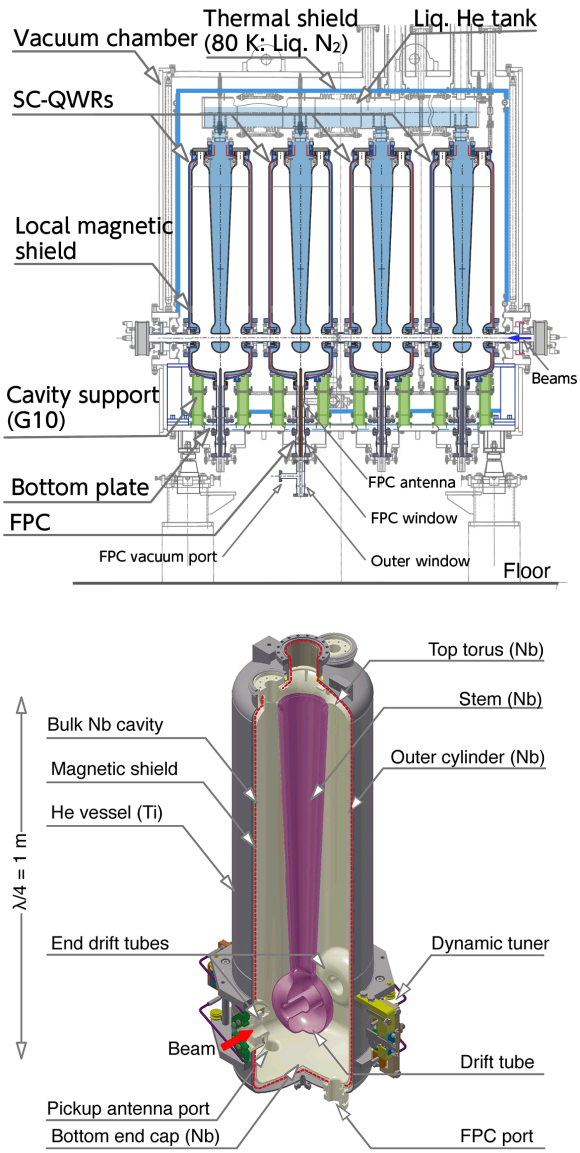

Figure 4: A schematic diagram of a full-CM (upper panel) and SC-QWR (lower panel) for the SRILAC. Liquid helium is stored in the blue region of the CM. The green pillars indicate insulating posts made of G10.

ISBN: 978-3-95450-234-9 ISSN: 2673-5504 doi:10.18429/JACoW-SRF2023-MOIXA04

Beam acceleration of the SRILAC was successfully performed on January 28, 2020. The details of beam commissioning and preparation are described in Ref. [20].

OPERATIONAL EXPERIENCE OF SRILAC

Operational History and Availability

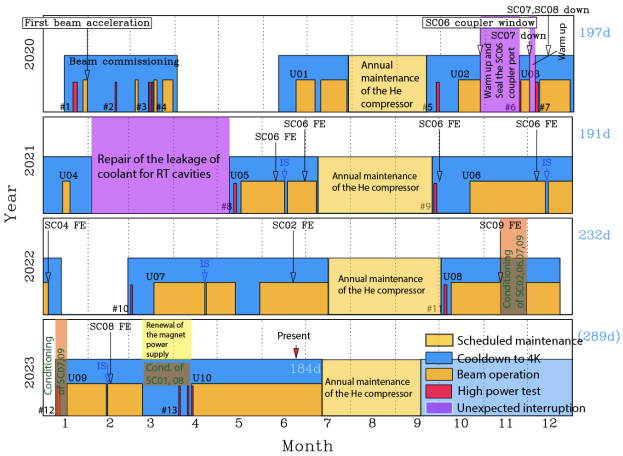

Figure 5: Operational history of the SRILAC.

SRILAC began supplying beams for user experiments soon after facility inspection in March 2020. Figure 5 shows the operational history of SRILAC since the first beam. The blue color indicates the cooling cycle of SRILAC and the orange color indicates the beam operation in the user experiments. Cooling was stopped for two months every summer for routine maintenance of the helium compressor and refrigerator.

SRILAC experienced vacuum leak problems twice because of a broken coupler window. The first vacuum leak occurred in the power coupler of SC05 during the warm-up process after the fourth cooling in November 2019 before beam commissioning. Thus, nine SC-QWRs were operational during the early days of operation. Subsequently, a second vacuum leak occurred from the coupler of SC06 on October 2020 during beam delivery. This problem forced the SRILAC to operate with eight SC-QWRs for a short period. However, this problem was successfully resolved by attaching an external vacuum window to the broken coupler, as described later, and all 10 SC-QWRs have been available for operation since the spring of 2021. The upstream room-temperature linac also experienced problems and was shut down for more than three months; however, since its repair, SRILAC has been able to operate stably without major problems. Consequently, SRILAC had ten user runs in its four years of operation.

Figure 6 shows the average daily downtime of the linac facility for the last three user runs. The overall availability of the linac facility is approximately 90%. Here, the availability is defined as the actual beam time divided by the scheduled beam time. The entry of SRILAC during downtime is mainly

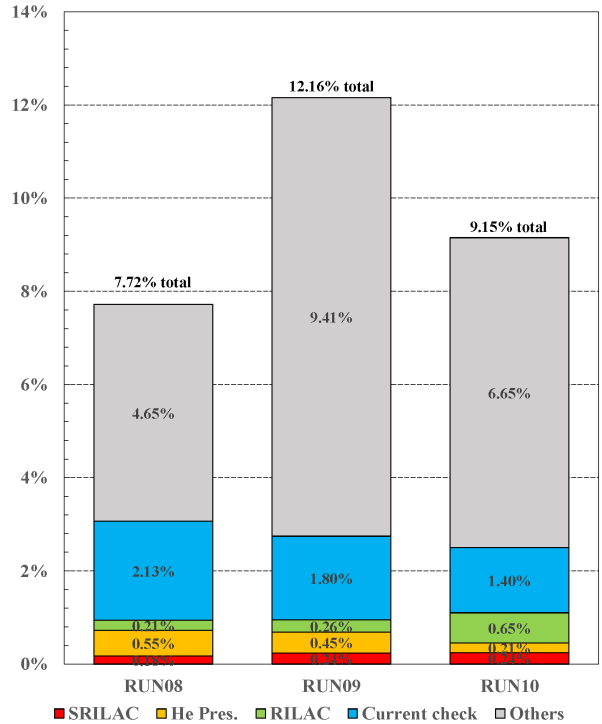

Figure 6: Average daily downtime of the linac facility. The item of Others includes the beam stop time due to the ion-source restart.

due to the unlocking of rf voltage and phase regulation. The entry of He pressure, which will be discussed later, was due to unwanted pressure fluctuations in the helium refrigerator. The combined value of these two entries is the SRILAC downtime. The availability of SRILAC has exceeded 99% in the last three runs, as listed in Table 1. The digital low-level circuit of the SRILAC is currently being modified, and further improvements in rf regulation are expected in the future.

Table 1: Availability of SRILAC in the Last Three User Runs

RUN No.	Period	Availability
RUN08	Oct. 11–Dec. 22, 2022	99.3%
RUN09	Jan. 18–Mar. 9, 2023	99.3%
RUN10	Apr. 16–Jun. 15, 2023	99.5%

Beam Tuning and Transport to Target

Beam tuning using SRILAC was performed as follows: First, after receiving the beam from the upstream room-temperature linac, the SRILAC was tuned by measuring the beam energy and position with BEPMs and by observing the response of the vacuum levels. Faraday cups and wire scanners were installed downstream of the HEBT. When transporting the beam to the user target, the beam width data measured by the wire scanner for different magnetic fields of the Q magnet were compared with the optics calculation [21].

ISBN: 978-3-95450-234-9 ISSN: 2673-5504 doi:10.18429/JACoW-SRF2023-MOIXA04

Figure 7 shows an example of a beam spot on the user target. The total tuning time after the ion source, including the room-temperature linac, was approximately 48 h for cold start. When the ion source is restarted or re-accelerated for user reasons, the parameters are already fixed; thus, beam tuning can be completed in approximately 12 h.

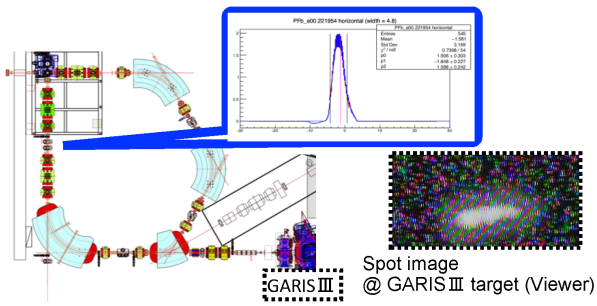

Figure 7: Example of the beam spot on the user target. The beam width information acquired by the wire scanner is used for the beam tuning.

To further increase the beam intensity in the future, we are currently attempting to estimate the beam phase ellipse non-destructively using BEPMs. The quadrupole moments obtained from the signals of the four BEPM electrodes of BEPMs are combined with the calculation results of the SRILAC transfer matrices. A reasonable phase ellipse estimation can be made [22] by considering the simulation results for the response of the BEPM signals to a low-beta heavy-ion beam, as shown in Fig. 8.

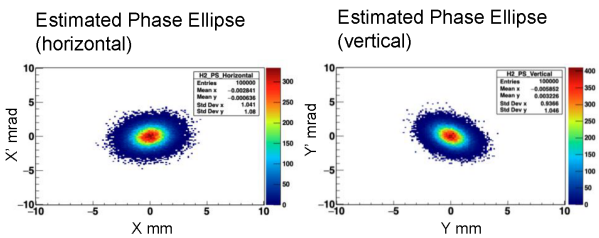

Figure 8: Estimated phase ellipse at the HEBT.

He Pressure Stability and Frequency Tuner

The absolute pressure of helium was stabilized at approximately ±0.2 kPa in the CMs by controlling each gas return valve. Because the frequency sensitivity to the pressure variation $\Delta f / \Delta P_{\mathrm{He}}$ is −2.0 Hz/hPa for the SC-QWR, the pressure fluctuation corresponds to a resonant frequency variation of ±4 Hz, which is considerably smaller than the operational bandwidth. However, periodic pressure fluctuations are observed in the helium refrigerator, as shown in the upper panel of Fig. 9. Although the process adjustment of the helium refrigerator reduced the frequency of pressure fluctuations, the problem of occasional large fluctuations remained, as indicated in the lower panel of Fig. 9. Cryomodules are affected by large pressure fluctuations, and the rf regulation is unlocked for several tens of seconds.

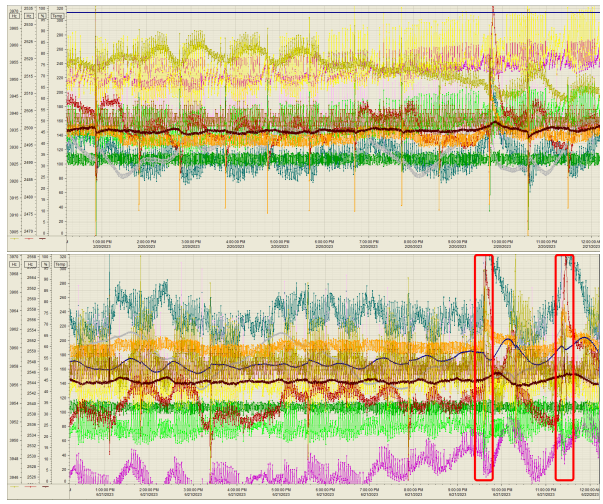

Figure 9: Process data trend of the helium refrigerator. The upper panel shows the trend before the process adjustment in Feb. 2023, and the lower panel shows the trend after the process adjustment in June 2023. The red boxes indicate occasional large pressure fluctuations.

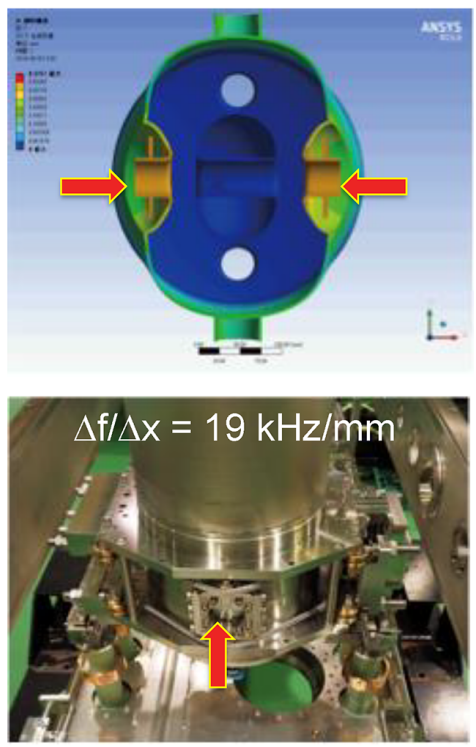

Figure 10: Frequency tuner of the SC-QWR for SRILAC. The upper panel shows a calculation result of deformation and the lower panel indicates a photo of the actual SC-QWR.

Figure 10 shows the calculation results for the deformation and a photograph of the frequency tuner for SRILAC [23]. The frequency of the SC-QWR is lowered by squeezing both beam ports to the cavity center using metallic wires, which are pulled by a stepping motor placed out of the cryomodule. The maximum allowance of the tuner is -14 kHz, and the

ISBN: 978-3-95450-234-9 ISSN: 2673-5504 doi:10.18429/JACoW-SRF2023-MOIXA04

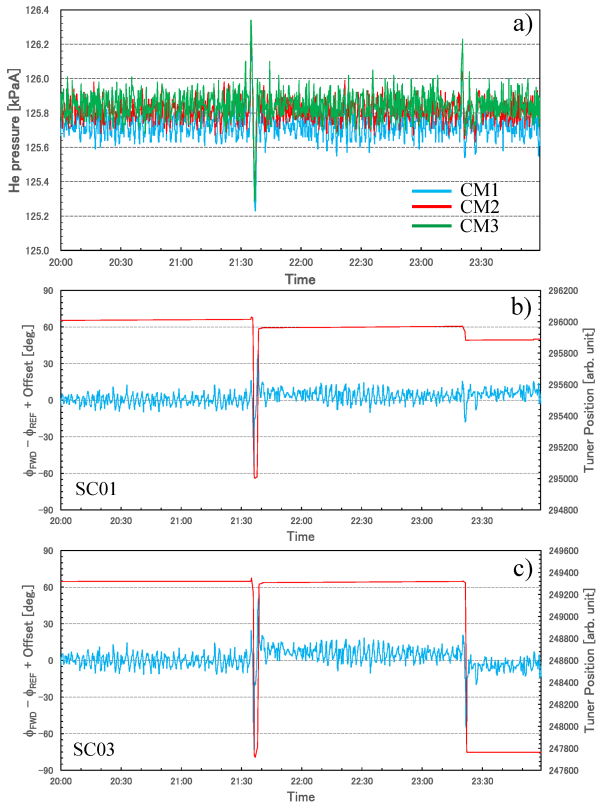

Figure 11: Helium pressure fluctuations in the CMs when the large fluctuations occur (a) and the corresponding automatic frequency compensation by the tuner of SC01 (b) and SC03 (c). In the panel (b) and (c), the blue line indicates the phase difference and the red line indicates the tuner position.

sensitivity is 19 kHz per millimeter. The frequency variation due to helium pressure fluctuation is automatically compensated by the proportional control of the tuner when the phase difference exceeds the dead zone of 15 °. The tuner is driven by the phase difference between the forward and reflected signals of the directional coupler. Figure 11 shows the helium pressure fluctuations in the CMs and the corresponding automatic frequency compensation by the tuner. The large fluctuations shown in Fig. 11 correspond to the red box in the lower panel of Fig. 9. Although automatic frequency compensation cannot keep up during large pressure fluctuations, the frequency tuner has operated stably for more than three years.

Field Emission and Pulse Conditioning

The field emission levels before opening the gate valves, one year after operation, and three years after operation are shown in Fig. 12. The onset voltage of field emission decreased over time. After the SC06 coupler window break, the emission levels of SC07 and SC08 increased significantly, and the performance of CM2 declined significantly. Furthermore, the emission levels of CM1 and CM3 gradually increased over the three years of operation. An increase in emission occurred suddenly during beam delivery; however,

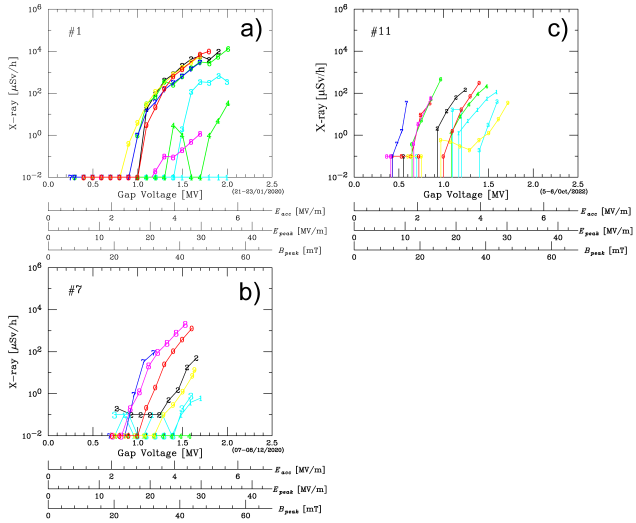

Figure 12: Emitted X-rays before opening the GVs (a), after one-year operation (b), and after three years of operation (c).

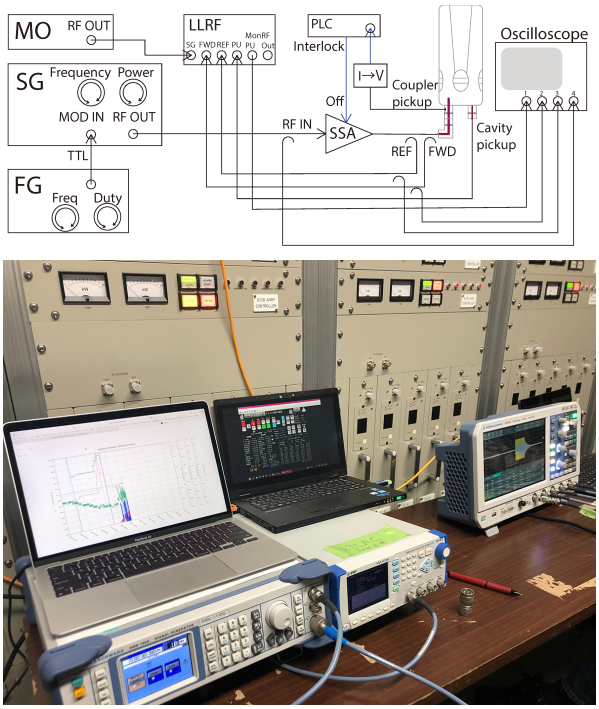

Figure 13: Block diagram and photo of the temporary setup for the pulse conditioning.

no beam loss or other events occurred at that time. Because the SRILAC continues to supply beams for user experiments, it is difficult to shut it down for long periods to perform maintenance. Therefore, we introduced pulse conditioning using a temporary setup [24].

Figure 13 shows a block diagram and a photograph of the temporary setup for pulse conditioning. The output of the signal generator is modulated by a function generator to produce a 20 msec width pulse, which is input directly to the solid-state amplifier. The interlock is activated by the forward, reflection, and pick-up signals inputted to the low-

ISBN: 978-3-95450-234-9 ISSN: 2673-5504 doi:10.18429/JACoW-SRF2023-MOIXA04

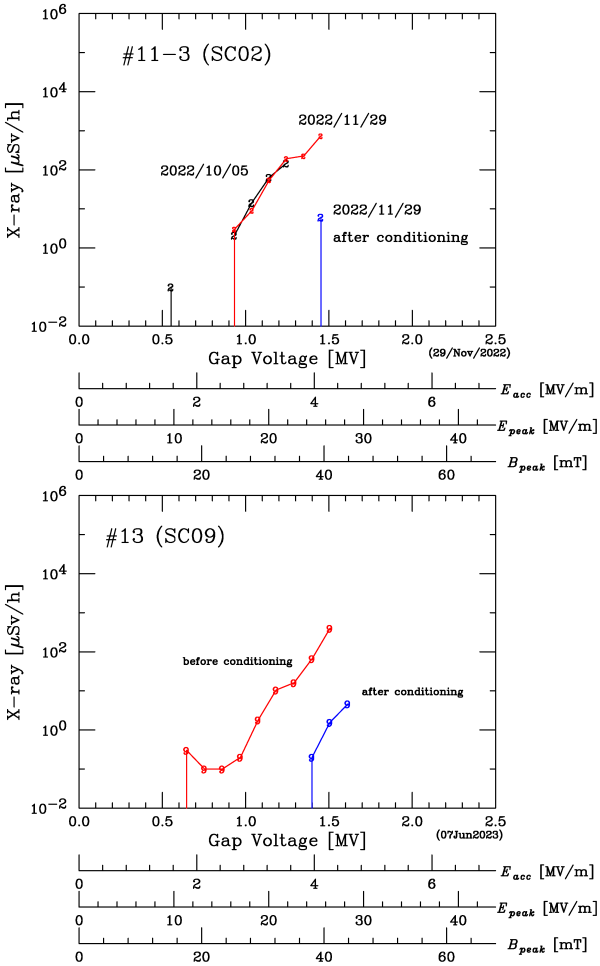

Figure 14: Effects of pulse conditioning.

level circuit and the electron pickup of the coupler. Initially, the pulse waveform of the cavity pick-up declined sharply due to multipacting in the early stage of pulse conditioning; however, multipacting was reduced as the conditioning progressed. Figure 14 shows examples of the pulse-conditioning results. In the SC02, X-ray emissions decreased from approximately 1 mSv/h to a few μSv/h after 40 min of pulse conditioning. A dramatic improvement was observed for SC09. Nine pulse-conditioning procedures were performed, all of which worked well. Thus, pulse conditioning was highly effective in the SRILAC for performance recovery.

New Couplers and SC-QWRs

As described in the previous section, the SRILAC experienced two vacuum leaks owing to the broken coupler window. The SRILAC couplers were designed to have a single room-temperature window. However, the original coupler was found to lower the window temperature by approximately 20 °C below the room temperature. Therefore, as reported at the last SRF conference, the insides of all the couplers were rusted owing to condensation. The two broken couplers were temporarily restored by attaching an external window and vacuum pumping, allowing all ten SC-QWRs to operate. We extended the temporary measures to all ten couplers, and they have been used without any problems for almost two years.

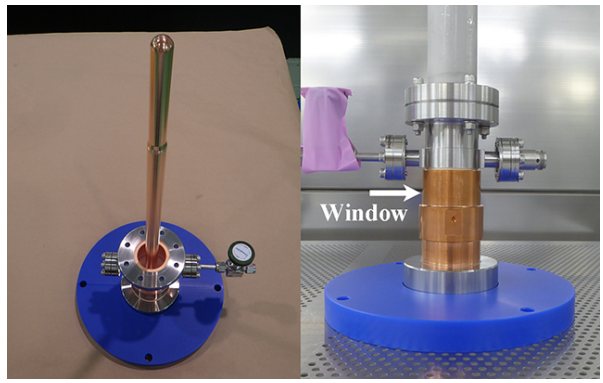

Figure 15: Fabricated new coupler with countermeasures.

Ten new couplers were fabricated using countermeasures to avoid cooling the vacuum window [25]. The poor thermal conductivity of the outer conductor resulted in the low window temperature. Consequently, the outer conductor between the window and the room-temperature thermal anchor changed to copper and the wall thickness increased. Figure 15 shows the photographs of the new power coupler for SRILAC. Only the component, including the vacuum window, was fabricated, and the outer conductor on the low-temperature side remained original. Currently, a residual gas analyzer is installed, and rf processing of the new couplers is performed in sequence.

We are also currently fabricating two SC-QWRs as spares. A photograph of the SC-QWR during the fabrication is shown in Fig. 16. Frequency pre-tuning and electron beam welding were completed, and two bulk niobium cavities are now in storage. Surface treatment, installation of a magnetic shield, and jacket welding will be performed in the future. We are beginning to prepare an HPR system at RIKEN that is as simple as possible.

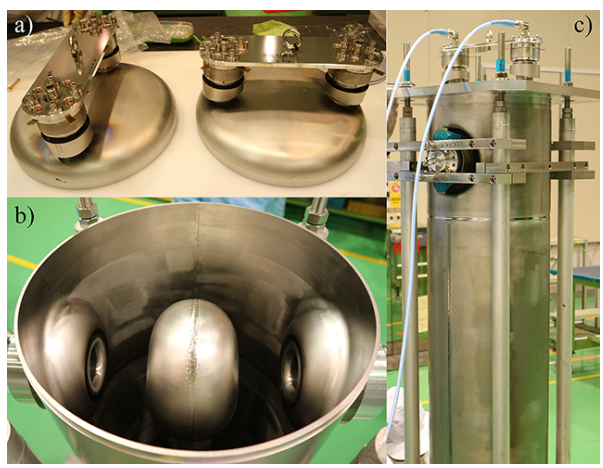

Figure 16: New SC-QWR in production. a) is the bottom plate, b) is the inside of SC-QWR, and c) is the measurement for frequency pre-tuning.

ISBN: 978-3-95450-234-9 ISSN: 2673-5504 doi:10.18429/JACoW-SRF2023-MOIXA04

SUMMARY

SRILAC has been in operation for four years. After overcoming the initial problems, SRILAC has been able to operate stably. Consequently, the availability of SRILAC exceeded 99%. The beam-tuning time is also reducing with the increase in the operational experience. Currently, the performance degradation of SRILAC can be recovered using pulse conditioning. The issue of occasional large pressure fluctuations in helium refrigerators requires further investigation. New couplers with countermeasures and spare SC-QWRs are being prepared, which are expected to shorten the work period required to resolve vacuum leakage and performance degradation.

ACKNOWLEDGEMENTS

The authors are grateful to Prof. E. Kako, H. Nakai, H. Sakai, and K. Umemori at KEK for their generous support in the construction of SRILAC. The authors would like to thank Prof. K. Saito at FRIB/MSU for technical advice on the design and assembly of the SRILAC. We would like to express our gratitude to the operators of SHI Accelerator Service Ltd. for their assistance.

REFERENCES

[1] Y. Yano, "The RIKEN RI Beam Factory Project: A status report", *Nucl. Instrum. Methods Phys. Res., Sect. B*, vol. 261, pp. 1009–1013, 2007. doi:10.1016/j.nimb.2007.04.174

[2] H. Okuno *et al.*, "Progress of RIBF accelerators", *Prog. Theor. Exp. Phys.*, vol. 2012, p. 03C002, 2012. doi:10.1093/ptep/pts046

[3] Y. Yano, "Recent Achievements at the RIKEN Ring Cyclotron", in *Proc. Cyclotrons'92*, Vancouver, Canada, Jul. 1992, paper I–21, pp. 102–105. https://jacow.org/c92/papers/i-21.pdf

[4] N. Inabe *et al.*, "Fixed-frequency ring cyclotron (fRC) in RIBF", in *Proc. Cyclotrons'04*, Tokyo, Japan, Oct. 2004, paper 18P15, pp. 200–202. https://jacow.org/c04/data/CYC2004_papers/18P15.pdf

[5] T. Mitsumoto *et al.*, "Construction of the fRC sector magnet for RIKEN RI Beam Factory", in *Proc. Cyclotrons'04*, Tokyo, Japan, Oct. 2004, paper 20P12, pp. 384–386. https://jacow.org/c04/data/CYC2004_papers/20P12.pdf

[6] N. Fukunishi *et al.*, "Acceleration of intense heavy ion beams in RIBF cascaded cyclotrons", in *Proc. 20th Int. Conf. on Cyclotrons and their Applications (Cyclotrons2013)*, Vancouver, Canada, Sep. 2013, pp. 1–6. https://jacow.org/CYCLOTRONS2013/papers/mo1pb01.pdf

[7] J. Ohnishi *et al.*, "Construction status of the RIKEN intermediate-stage ring cyclotron (IRC)", in *Proc. Cyclotrons'04*, Tokyo, Japan, Oct. 2004, paper 18P14, pp. 197–199. https://jacow.org/c04/data/CYC2004_papers/18P14.pdf

[8] H. Okuno *et al.*, "The superconducting ring cyclotron in RIKEN", *IEEE Trans. Appl. Supercond.*, vol. 17, pp. 1063–1068, 2007. doi:10.1109/TASC.2007.899864

[9] M. Odera *et al.*, "Variable frequency heavy-ion linac, RILAC", *Nucl. Instrum. Methods Phys. Res., Sect. A*, vol. 227, pp. 187–195, 1984. doi:10.1016/0168-9002(84)90121-9

[10] O. Kamigaito *et al.*, "Construction of a booster linac for the RIKEN heavy-ion linac", *Rev. Sci. Instrum.*, vol. 76, p. 013306, 2005. doi:10.1063/1.1834708

[11] K. Yamada *et al.*, "Beam Commissioning and Operation of New Linac Injector for RIKEN RI-beam Factory", in *Proc. IPAC'12*, New Orleans, LA, USA, May 2012, paper TUOBA02, pp. 1071–1073. https://jacow.org/IPAC2012/papers/tuoba02.pdf

[12] K. Suda *et al.*, "Design and construction of drift tube linac cavities for RIKEN RI Beam Factory", *Nucl. Instrum. Methods Phys. Res., Sect. A*, vol. 722, pp. 55–64, 2013. doi:10.1016/j.nima.2013.04.007

[13] A. Goto *et al.*, "Injector AVF cyclotron at RIKEN", in *Proc. Cyclotrons'89*, Berlin, Germany, May 1989, paper B–07, pp. 51–54. https://jacow.org/c89/papers/b-07.pdf

[14] K. Morita *et al.*, "New Result in the Production and Decay of an Isotope, ^{278}113, of the 113th Element", *J. Phys. Soc. Jpn.*, vol. 81, p. 103201, 2012. doi:10.1143/JPSJ.81.103201

[15] O. Kamigaito *et al.*, "Present Status and Future Plan of RIKEN RI Beam Factory", in *Proc. IPAC'16*, Busan, Korea, May 2016, pp. 1281–1283. doi:10.18429/JACoW-IPAC2016-TUPMR022

[16] N. Nagatomo *et al.*, "New 28-GHz Superconducting ECR Ion Source for Synthesizing New Super Heavy Elements of Z>118", in *Proc. ECRIS'18*, Catania, Italy, Sep. 2018, pp. 53–57. doi:10.18429/JACoW-ECRIS2018-TUA3

[17] N. Sakamoto *et al.*, "Construction Status of the Superconducting Linac at the RIKEN Radioactive Isotope Beam Facility", in *Proc. LINAC'18*, Beijing, China, Sep. 2018, pp. 620–625. doi:10.18429/JACoW-LINAC2018-WE2A03

[18] T. Watanabe *et al.*, "Commissioning of the Beam Energy Position Monitoring System for the Superconducting RIKEN Heavy-Ion Linac", in *Proc. IBIC'20*, Santos, Brazil, Sep. 2020, pp. 295–302. doi:10.18429/JACoW-IBIC2020-FRA004

[19] H. Imao *et al.*, "Non-Evaporable Getter-Based Differential Pumping System for SRILAC at RIBF", in *Proc. SRF'19*, Dresden, Germany, Jun.-Jul. 2019, pp. 419–423. doi:10.18429/JACoW-SRF2019-TUP013

[20] K. Yamada *et al.*, "Successful Beam Commissioning of Heavy-ion Superconducting Linac at RIKEN", in *Proc. SRF'21*, East Lansing, MI, USA, Jun.-Jul. 2021, pp. 167. doi:10.18429/JACoW-SRF2021-MOOFAV01

[21] T. Nishi *et al.*, "Beam Acceleration with the Upgraded Riken Heavy-Ion Linac", in *Proc. HB'21*, Batavia, USA, Oct. 2021, paper THBC1, p. 231. doi:10.18429/JACoW-HB2021-THBC1

[22] T. Nishi *et al.*, "Development of Non-Destructive Beam Envelope Measurements in SRILAC with Low Beta Heavy Ion Beams Using BPMs", presented at SRF'23, Grand Rapids, MI, USA, Jun. 2023, paper MOPMB086, this conference.

ISBN: 978-3-95450-234-9 ISSN: 2673-5504 doi:10.18429/JACoW-SRF2023-MOIXA04

[23] K. Suda *et al.*, "New Frequency-Tuning System and Digital LLRF for Stable and Reliable Operation of SRILAC", in *Proc. SRF'21*, East Lansing, MI, USA, Jun.-Jul. 2021, p. 666. doi:10.18429/JACoW-SRF2021-WEPTEV013

[24] N. Sakamoto *et al.*, "Degradation and Recovery of Cavity Performance in SRILAC Cryomodules at RIBF", presented at SRF'23, Grand Rapids, MI, USA, Jun. 2023, paper WEPWB085, this conference.

[25] K. Ozeki *et al.*, "Present Status of RIKEN Power Couplers for SRILAC", presented at SRF'23, Grand Rapids, MI, USA, Jun. 2023, paper WEPWB101, this conference.